regions (such as Amazon Basin and Western Pacific) of enhanced D_P, but it is also larger over land, where it averages H_P = 6.9 km, than over the ocean, with H_P = 5.1 km. Both numbers fall within the range of H_P = 5 to 10 km estimated in (*1*) and are consistent with the fact that convective motions tend to be more intense over land over the ocean. In addition to the land-sea contrast, other geographic variations of H_P can be noted in Fig. 3, including high values over semiarid regions (Australia and Northern Africa) and over high-altitude regions (Himalaya and Andes). High values of H_P are also found over Southwest Mexico and Peru during JJA and over northern Africa during December, January, and February (DJF), corresponding to the dry season in these locations. These high values of H_P are associated with intermittent deep convection in an otherwise dry atmosphere. In such conditions, a large fraction of the precipitation reevaporates before reaching the ground. And although such reevaporating precipitation does not contribute to the rainfall at the surface, it does increase the amount of frictional dissipation within the atmospheric column, leading to higher value of the precipitation scale height in these regions. Conversely, the lowest H_P values occur along the eastern coast of South America and Africa, in regions characterized by shallow convection.

Our analysis of precipitation profiles from satellite measurements confirms that precipitation-induced dissipation is a major dissipative mechanism in Earth's atmosphere, with an average dissipation rate of 1.8 W m^{-2} for the tropical regions for the period of 1999 to 2007. Because it has been argued (*14*, *16*) that the TRMM PR instrument on which this study is based tends to underestimate the amount of precipitation, the actual value of the dissipation is likely to be somewhat larger than that reported here. Additional observations, either space-born or ground-based radars, could provide additional data to refine this estimate. Newly available retrievals from CloudSat Cloud Profiling Radar (*17*, *18*) should make it possible to extend the current analysis to include the extratropics. As Earth warms as a result of increased greenhouse gas concentration, both the amount of precipitation and the average height at which condensation occurs should increase. Both of these changes imply an increase in the precipitation-induced dissipation. A better understanding of the hydrological cycle and of the dissipation associated with it, in particular how these may be affected by natural or anthropogenic climate change, would provide new insights on how the intensity of the atmospheric circulation may vary.

References and Notes

1. O. Pauluis, V. Balaji, I. M. Held, *J. Atmos. Sci.* **57**, 989 (2000).
2. E. N. Lorenz, *The Nature and Theory of the General Circulation of the Atmosphere* (World Meteorological Organization, Geneva, 1967).
3. K. A. Emanuel, M. Bister, *J. Atmos. Sci.* **53**, 3276 (1996).
4. N. O. Rennó, A. P. Ingersoll, *J. Atmos. Sci.* **53**, 572 (1996).
5. R. Goody, *J. Atmos. Sci.* **60**, 2827 (2003).
6. O. Pauluis, I. M. Held, *J. Atmos. Sci.* **59**, 125 (2002).
7. O. Pauluis, *J. Atmos. Sci.* **68**, 91 (2011).
8. O. Pauluis, I. M. Held, *J. Atmos. Sci.* **59**, 140 (2002).
9. O. Pauluis, in *Non-Equilibrium Thermodynamics and the Production of Entropy*, A. Kleidon, R. D. Lorenz, Eds. (Springer-Verlag, Berlin, 2005), pp. 107–119.
10. J. P. Peixoto, A. H. Oort, M. de Almeida, A. Tomé, *J. Geophys. Res.* **96**, 10981 (1991).
11. J. P. Peixoto, A. H. Oort, *Physics of Climate* (American Institute of Physics, New York, 1992).
12. E. Becker, *Mon. Weather Rev.* **131**, 508 (2003).
13. T. Iguchi, T. Kozu, R. Meneghini, J. Awaka, A. K. Okamoto, *J. Appl. Meteorol.* **39**, 2038 (2000).
14. T. Bellerby, M. Todd, D. Kniveton, C. Kidd, *J. Appl. Meteorol.* **39**, 2115 (2000).
15. T. Iguchi *et al.*, *J. Meteorol. Soc. Jpn.* **87A**, 1 (2009).
16. K. P. Bowman, *J. Clim.* **18**, 178 (2005).
17. G. L. Stephens *et al.*, *Bull. Am. Meteorol. Soc.* **83**, 1771 (2002).
18. C. Mitrescu, T. L'Ecuyer, J. Haynes, S. Miller, J. Turk, *J. Appl. Meteorol. Climatol.* **49**, 991 (2010).

Acknowledgments: The TRMM 3A25 data were obtained from the TRMM Science Data and Information System (TSDIS) at Goddard Space Flight Center, NASA. The authors are thankful to A. Ackerman, A. Del Genio, G. Tselioudis, and A. Fridlind for their comments on a previous version of this manuscript. This work has been supported by NSF grants ATM-0545047 and AGS-0944058.

27 October 2011; accepted 25 January 2012
10.1126/science.1215869

Collapse of Classic Maya Civilization Related to Modest Reduction in Precipitation

Martín Medina-Elizalde and Eelco J. Rohling*

The disintegration of the Classic Maya civilization in the Yucatán Peninsula and Central America was a complex process that occurred over an approximately 200-year interval and involved a catastrophic depopulation of the region. Although it is well established that the civilization collapse coincided with widespread episodes of drought, their nature and severity remain enigmatic. We present a quantitative analysis that offers a coherent interpretation of four of the most detailed paleoclimate records of the event. We conclude that the droughts occurring during the disintegration of the Maya civilization represented up to a 40% reduction in annual precipitation, probably due to a reduction in summer season tropical storm frequency and intensity.

Ever since the discovery of the ancient Maya civilization, climate change has been invoked as a causal factor to explain its collapse centuries before the first arrival of Europeans on the American continent (*1*, *2*). It has since become well established that the disintegration of the Classic Maya Civilization was a complex process occurring from around 800 to 1000 A.D. [known as the Terminal Classic Period (TCP)] (*1*–*7*). Despite evidence suggesting that climate change does not fully explain the complex geographic and sociopolitical events of the TCP (*2*, *8*), paleoclimate records and archaeological evidence suggest that the TCP was punctuated by a series of drought events (*9*–*15*) that probably triggered significant societal disruptions at this time (*16*, *17*). Unfortunately, paleoclimate records have been interpreted largely in qualitative terms, and no coherent interpretative framework of these records exists. The TCP drought signals suggested by paleoclimate records are not far outside the amplitude of those preceding this time interval, when the Maya civilization flourished. Perhaps the magnitude of these droughts was rather modest despite the large associated environmental and societal disruptions.

Here we develop the first coherent, quantitative view of the four best-dated and best-resolved paleoclimate records from the Yucatán Peninsula (YP) (Figs. 1 and 2). We evaluate YP lake responses to perturbations to the seasonal precipitation cycle using a straightforward isotope mass balance model, for comparison with environmental patterns suggested by these records. This approach provides a single consistent interpretative framework for all records considered and thus for a quantitative cross-validation of the environmental signals.

The key YP paleoclimate records that we consider (Fig. 2) show similar environmental patterns over the TCP, which are near to synchronous within chronological uncertainties. The high-resolution U-Th–dated stalagmite (named Chaac after the Maya god of rain) $\delta^{18}O$ record represents variability in the annual mean $\delta^{18}O$ of precipitation and reveals a succession of extended drought periods interrupted by brief recoveries (*14*) (Fig. 2A). The Lake Chichancanab gastropod and Punta Laguna ostracod $\delta^{18}O$ records show

National Oceanography Centre, University of Southampton, Southampton, UK.

*Present address: Centro de Investigación Científica de Yucatán, UCIA, Cancún, México.

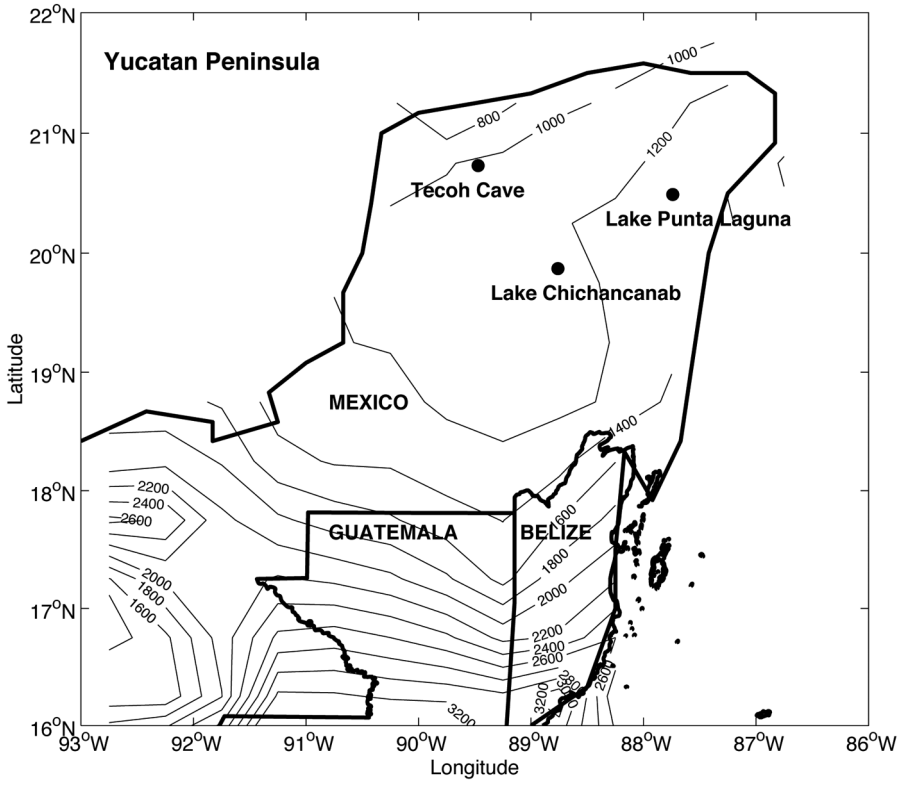

Fig. 1. Map of the YP, including the countries of México, Belize, and Guatemala. Contours represent total annual precipitation isolines (in millimeters per year). The locations of the stalagmite Chaac, the town of Tecoh (20°45′N, 89°28′W, 20 m above sea level); Lake Chichancanab (19°52′N, 88°46′W); and Lake Punta Laguna (20°38′N, 87°37′W, 18 m above sea level) are indicated (black circles).

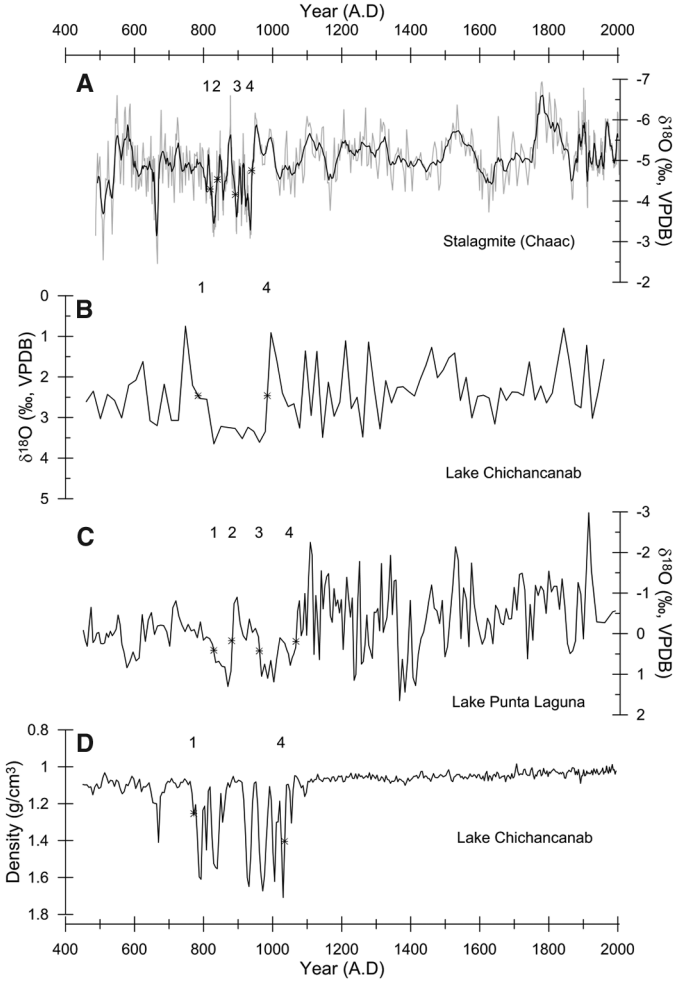

Fig. 2. YP climate records spanning the past 1500 years. (**A**) Stalagmite Chaac $\delta^{18}O$ record of changes in the $\delta^{18}O$ composition of rainfall (*14*). VPDB, Vienna Pee Dee belemnite standard. (**B**) Lake Chichancanab *Pyrgophorus coronatus* $\delta^{18}O$ record, reflecting changes in the evaporation/precipitation isotope balance (*9*). (**C**) Lake Punta Laguna ostracod *Cytheridella ilosvayi* $\delta^{18}O$ record, also reflecting this isotope balance (*10*). (**D**) Lake Chichancanab sediment density record, reflecting gypsum precipitation and lake drawdown (*15*). In (A) to (D), symbols and numbers (1 to 4) represent tiepoints used in graphic tuning of the lake records to the Chaac $\delta^{18}O$ record (*18*) (Fig. 3) The TCP isotopic anomalies do not significantly exceed those bounding the TCP, suggesting modest changes in the balance of evaporation and precipitation.

changes in the balance between the supply of light isotopes by precipitation and their removal by evaporation (*9*, *10*) (Fig. 2, B and C). Last, the Lake Chichancanab sediment density record (Fig. 2D) reflects gypsum supersaturation due to evaporative drawdown and concentration of the lake, which even today is at gypsum saturation (*15*). The Lake Chichancanab gastropod $\delta^{18}O$ record lacks resolution relative to all the other records, which explains why the brief drought recoveries inside the TCP are not visible (*10*, *14*) (Fig. 2).

The underlying processes driving the patterns and amplitudes of the YP environmental records during the TCP are evaluated with an isotope mass balance model set up for Lake Chichancanab (*18*). Our model successfully reproduces: (i) a steady modern annual mean lake level, with superimposed seasonal variability; (ii) mass-balanced isotope fluxes; and (iii) an equilibrium lake water $\delta^{18}O$ of 3.9 per mil (‰) that agrees with observed $\delta^{18}O$ values for Lake Chichancanab (*9*, *19*, *20*). Thus, our straightforward isotope model offers a realistic approximation for the assessment of lake sensitivity to perturbations of the precipitation cycle.

Modeled lake variability through the TCP needs to meet the following conditions indicated by the paleoclimate records shown in Fig. 2: (i) significant lake drawdown but not fully desiccated, as evidenced by the uninterrupted organic calcite sequences; and (ii) a total lake $\delta^{18}O$ amplitude fluctuation of ~ ±2.5‰. This platform is used to evaluate the implication for YP lake mass and isotope balance of two different scenarios of perturbation of the seasonal precipitation cycle and $\delta^{18}O$ of precipitation (δ_P). In these scenarios,

precipitation (P) is perturbed by a constant fraction for every month of the wet season, which we take to be the 5 months (June to October) during which P today exceeds 100 mm (*21*). Every time we impose a perturbation of P, we impose proportional changes in δ_P, in accordance with the amount effect relationship between modern P and δ_P values [$\delta_P/\Delta P$ = –0.0234‰/mm; regression coefficient (R^2) = 0.80] (*18*).

The first scenario that we test is that the TCP droughts reflect a persistent summer season shift of the convective activity away from the YP (*13*). In this scenario, we reduce monthly summer precipitation to values where the mean summer precipitation becomes equal to the mean winter precipitation, which effectively means that the area is "locked" in a winter precipitation mode. Using the amount effect relationship, δ_P is then adjusted proportionally. As a result of such a perturbation of summer precipitation, Lake Chichancanab fully desiccates in 14 years, which is within the time span of the two longest TCP droughts (*14*) (Fig. 2A). This is in conflict with evidence of the continuous existence of Lakes Chichancanab and Punta Laguna throughout the TCP. Furthermore, modeled lake isotope values become extremely positive, in excess of 10‰, far exceeding recorded isotope anomalies (Fig. 2, B and C). Finally, this scenario would imply a mean isotope shift of 2.5‰ in the Chaac $\delta^{18}O$ record as opposed to the observed 1‰ (Fig. 2A).

In the second scenario, we use our isotope mass balance model to simulate the development of Lake Chichancanab as a function of weaker perturbations in summer precipitation (Fig. 3). We maintain the modern annual rainfall cycle but shift the summer precipitation amount and therefore mean summer season δ_P so that the annual mean δ_P changes in accordance to the interannual $\delta^{18}O$ precipitation anomalies reflected by Chaac (*18*) (Fig. 3A). Modeled annual mean lake $\delta^{18}O$ anomalies that result from these changes in P and δ_P are in close agreement with observations from Lake Chichancanab and especially Lake Punta Laguna, thus validating the imposed precipitation shifts (*18*) (Fig. 3, B and C).

Calculated summer precipitation reductions associated with the Chaac $\delta^{18}O$ anomalies range from 30 to 50%, which equate to annual mean P reductions of 25 to 40% (*18*) (Fig. 3A). Modeled Lake Chichancanab water level is reduced by 30% during the two longest and most severe droughts centered at 830 and 928 C.E. (*14*) (Fig. 3C). Given that the lake today is close to gypsum saturation already (*15*), these water level reductions are consistent with supersaturation and precipitation of gypsum, in agreement with the Lake Chichancanab density record (*15*) (Fig. 3C). The equal magnitude of all gypsum precipitation events during the TCP contrasts with more subtle variations in modeled lake depth, although the timing of these events is very similar between the two records. We thus infer that gypsum precipitation represents a nonlinear threshold response to lake level (Fig. 3D).

We find that available paleoclimate records support a coherent and consistent interpretation of considerable reductions in precipitation during the TCP, but not as severe as would be implied by previously proposed mechanisms (*13*). If these repeated episodes of drier climate had a significant role in the fate of the Classic Maya civilization, as suggested by archaeological evidence (*16*, *17*), then this would imply that the ecological carrying capacity of the YP is highly sensitive to precipitation reductions. Indeed, such sensitivity to relatively minor changes in precipitation would agree with observations that variations in interannual precipitation today, mainly associated with the frequencies of tropical storms and depressions, significantly affect the groundwater table in the YP (*20*). Our estimated TCP rainfall reductions are within the range of rainfall deficits over the YP as projected by climate models for the end of this century (*22*, *23*).

Finally, we note that the TCP drought episodes are predominantly characterized by the absence of light (summer) isotope values (*14*). Today, the lightest isotope excursions are associated with the large precipitation fluxes of tropical storms and hurricanes (*20*, *24*, *25*), and the region depends on tropical depressions, storms, and hurricanes to maintain a positive net water balance and avoid desiccation (*24*, *26*, *27*). We suggest, therefore, that the droughts associated with the disintegration of the Maya civilization may have been triggered by a reduced frequency and intensity of cyclones over the YP. The inferred P reductions during the TCP are within the range associated with one to three tropical storms (*26*, *28*, *29*). Our interpretation of the TCP droughts may be validated by future research focused on detailed dating of storm deposits around the Yucatán and/or monthly resolved paleotempest records [such as those from speleothems (*25*)].

The modest reductions in precipitation associated with the end of the Classic Maya civilization highlight the critical sensitivity of the ecological carrying capacity of the YP to even small shifts in the region's hydrological budget, such as those projected for the near future (*22*, *23*). This study shows that it is possible to reconstruct the geographical pattern of precipitation evolution in México and Central America by increasing the coverage of stalagmite and lake records. Given the now apparent temporal complexity in the record of precipitation change (*14*) (Fig. 3A), we expect spatial complexities also.

This study advances the debate from one centered around qualitative interpretations of intense droughts to one around quantitative estimations

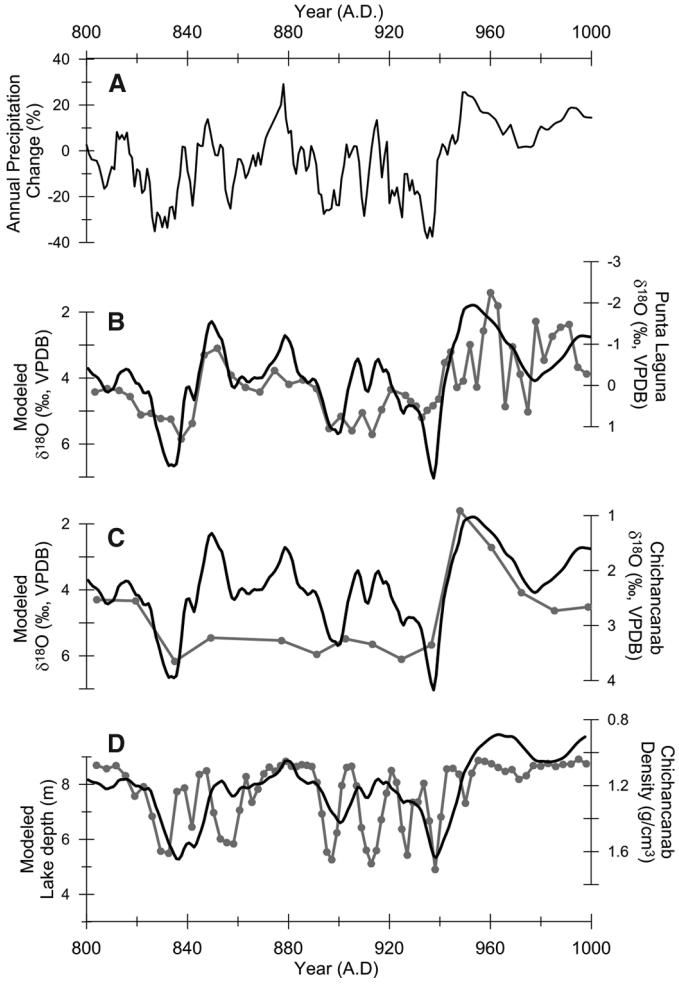

Fig. 3. (**A**) TCP annual precipitation percent changes, reflecting Chaac $\delta^{18}O$ anomalies, used in the isotope mass balance model for Lake Chichancanab. (**B** and **C**) Comparison of lake $\delta^{18}O$ evolutions during the TCP suggested by modeled (black) and paleoclimate (gray line with symbols) records, from Lake Chichancanab (B) and Punta Laguna (C). (**D**) Comparison between modeled lake level (black) and Lake Chichancanab sediment density record (gray with symbols), reflecting gypsum precipitation and lake drawdown. The lake paleoclimate records were graphically tuned to the stalagmite Chaac $\delta^{18}O$ record (*18*). Tuning tiepoints are shown in Fig. 2.

that support the scenario of drought of subtle variability with high impact. In addition, the data and modeling support an interpretation of decreased rainfall during the summer, associated with a reduction in the severity and frequency of tropical storms. This study suggests that there is substantial potential for establishing a relationship between the actual climatic variability over the region and the spatially complex historical events (*30*) that shaped the demise of the Maya civilization.

References and Notes

1. L. Schele, M. E. Miller, in *The Blood of Kings: Dynasty and Ritual in Maya Art*, G. I. Braziller, Ed. (George Braziller, New York, and Kimbell Art Museum, Fort Worth, TX, 1986), p. 335.
2. A. A. Demarest, P. M. Rice, D. S. Rice, in *The Terminal Classic in the Maya Lowlands: Collapse, Termination, and Transformation*, A. A. Demarest, P. M. Rice, D. S. Rice, Eds. (Univ. Press of Colorado, Boulder, CO, 2004), pp. 1–11.
3. T. P. Culbert, in *Precolumbian Population History in the Maya Lowlands*, T. P. Culbert, D. S. Rice, Eds. (Univ. of New Mexico Press, Albuquerque, NM, 1990), p. 395.
4. W. J. Folan, *Información Universidad Autónoma Ciudad de México (UACM)* **13**, 122 (1988).
5. B. L. Turner, in *Population Reconstruction for the Central Maya Lowlands: 1000 B.C. to A.D. 1500*, T. P. Culbert, D. S. Rice, Eds. (Univ. of New Mexico Press, Albuquerque, NM, 1990), pp. 301–324.
6. T. P. Culbert, L. J. Kosakowsky, R. E. Fry, W. A. Haviland, in *Precolumbian Population History in the Maya Lowlands*, T. P. Culbert, D. S. Rice, Eds. (Univ. of New Mexico Press, Albuquerque, NM, 1990), pp. 103–121.
7. P. A. Andrews, E. W. Andrews, F. R. Castellanos, *Ancient Mesoam.* **14**, 151 (2003).
8. J. Aimers, D. A. Hodell, *Nature* **479**, 44 (2011).
9. D. A. Hodell, J. H. Curtis, M. Brenner, *Nature* **375**, 391 (1995).
10. J. H. Curtis, D. A. Hodell, M. Brenner, *Quat. Res.* **46**, 37 (1996).
11. J. H. Curtis *et al.*, *J. Paleolimnol.* **19**, 139 (1998).
12. M. F. Rosenmeier, D. A. Hodell, M. Brenner, J. H. Curtis, T. P. Guilderson, *Quat. Res.* **57**, 183 (2002).
13. G. H. Haug *et al.*, *Science* **299**, 1731 (2003).
14. M. Medina-Elizalde *et al.*, *Earth Planet. Sci. Lett.* **298**, 255 (2010).
15. D. A. Hodell, M. Brenner, J. H. Curtis, *Quat. Sci. Rev.* **24**, 1413 (2005).
16. G. E. Braswell *et al.*, in *The Terminal Classic in the Maya Lowlands: Collapse, Transition, and Transformation*, A. A. Demarest, P. M. Rice, D. S. Rice, Eds. (Univ. Press of Colorado, Boulder, CO, 2004), pp. 162–194.
17. K. Carmean, N. Dunning, J. K. Kowalski, in *The Terminal Classic in the Maya Lowlands: Collapse, Transition, and Transformation*, A. A. Demarest, P. M. Rice, D. S. Rice, Eds. (Univ. Press of Colorado, Boulder, CO, 2004), pp. 424–449.
18. Materials and methods are available as supporting material on *Science* Online.
19. A. Covich, M. Stuiver, *Limnol. Oceanogr.* **19**, 683 (1974).
20. E. Perry, G. Velazquez-Oliman, A. R. Socki, *Hydrogeology of the Yucatán Peninsula*, 21st Symposium on Plant Biology, Arturo Gomez Pompa, Scott Fedick, Eds. (Haworth Press, Binghamton, NY, 2003), pp. 115–138.
21. CONAGUA, Servicio meteorológico nacional, México; available at http://smn.cna.gob.mx/ (2011).
22. J. H. Christensen *et al.*, *Regional Climate Projections. Climate Change 2007: The Physical Science Basis* (Cambridge Univ. Press, Cambridge, 2007).
23. A. V. Karmalkar, R. S. Bradley, H. F. Diaz, *Clim. Dyn.* **37**, 605 (2011).
24. R. J. Lawrence, D. S. Gedzelman, *Geophys. Res. Lett.* **23**, 527 (1996).
25. A. B. Frappier, D. Sahagian, S. J. Carpenter, L. A. Gonzalez, B. R. Frappier, *Geology* **35**, 111 (2007).
26. W. K. Michener, E. R. Blood, K. L. Bildstein, M. M. Brinson, L. R. Gardener, *Agric. Appl.* **7**, 770 (1997).
27. H. Jiang, E. J. Zipser, *J. Clim.* **23**, 1526 (2010).
28. F. N. Scatena, M. C. Larsen, *Biotropica* **23**, 317 (1991).
29. NOAA, National Weather Service/National Hurricane Center; available at: www.nhc.noaa.gov/ (2011).
30. R. B. Gill, *The Great Maya Droughts: Water, Life, and Death* (Univ. of New Mexico Press, Albuquerque, NM, 2000).

Acknowledgments: This paper contributes to UK Natural Environment Research Council projects NE/C003152/1, NE/I009906/1, and NE/H004424/1. We thank two anonymous reviewers for their valuable comments and suggestions.

Supporting Online Material

www.sciencemag.org/cgi/content/full/335/6071/956/DC1
Materials and Methods
SOM Text
Table S1
References (*31*–*34*)

14 November 2011; accepted 23 January 2012
10.1126/science.1216629

Evolution of the Earliest Horses Driven by Climate Change in the Paleocene-Eocene Thermal Maximum

Ross Secord,[1,2]* Jonathan I. Bloch,[2] Stephen G. B. Chester,[3] Doug M. Boyer,[4] Aaron R. Wood,[5,2] Scott L. Wing,[6] Mary J. Kraus,[7] Francesca A. McInerney,[8] John Krigbaum[9]

Body size plays a critical role in mammalian ecology and physiology. Previous research has shown that many mammals became smaller during the Paleocene-Eocene Thermal Maximum (PETM), but the timing and magnitude of that change relative to climate change have been unclear. A high-resolution record of continental climate and equid body size change shows a directional size decrease of ~30% over the first ~130,000 years of the PETM, followed by a ~76% increase in the recovery phase of the PETM. These size changes are negatively correlated with temperature inferred from oxygen isotopes in mammal teeth and were probably driven by shifts in temperature and possibly high atmospheric CO_2 concentrations. These findings could be important for understanding mammalian evolutionary responses to future global warming.

Interest in how organisms respond to climate change has intensified in recent years with projected warming of ~2° to 4°C over the next century (*1*). Although models can be developed to predict evolutionary responses to warming of this magnitude, empirical examples must be drawn from fossil or historical records. Here we report a dramatic example of shifts in body size in the earliest known horses (family Equidae) during the Paleocene-Eocene Thermal Maximum (PETM) (~56 million years ago). The PETM is recognized in marine and continental records by an abrupt negative carbon isotope excursion (CIE) that lasted ~175 thousand years (ky), caused by the release of thousands of gigatons of carbon to the ocean-atmosphere system (*2*, *3*). Some marine records suggest that although $\delta^{13}C$ values shifted rapidly at the onset of the CIE in 21 ky or less (*2*), temperature increase was slower, peaking 60 ky or more into the CIE (*4*) at ~5° to 10°C above pre-CIE levels (*5*, *6*). We use oxygen isotope values in mammal teeth as a proxy for local temperature change in the continental interior of North America, and we show that equid body size during the PETM was negatively correlated with temperature.

In extant mammals and birds (endotherms), closely related species or populations within a species are generally smaller-bodied at lower latitudes, where ambient temperature is greater (*7*). This relationship, known as Bergmann's rule, is followed by ~65 to 75% of studied extant mammals (*8*, *9*). The cause of Bergmann's rule is usually attributed to thermoregulation and the optimization of body size (*10*) and/or the availability of food resources related to primary productivity (*11*). Bergmann's rule predicts that average mammalian body size should decrease with warming climate, and smaller size in endotherms has even been suggested as a third "universal" response to warming, along with changes in phenology and species distribution (*10*). Declining body size has been attributed to warming over decadal and millennial scales in some living endotherms (*12*, *13*), but many counterexamples also exist (*10*). Furthermore, it is difficult to distinguish natural selection (genetic change) from ecophenotypic plasticity (morphological response

[1]Department of Earth and Atmospheric Sciences, University of Nebraska, Lincoln, NE 68588, USA. [2]Florida Museum of Natural History, University of Florida, Gainesville, FL 32611–7800, USA. [3]Department of Anthropology, Yale University, New Haven, CT, 06520, USA. [4]Department of Anthropology and Archaeology, Brooklyn College, City University of New York, New York, NY 11210, USA. [5]Department of Geology and Geological Engineering, South Dakota School of Mines and Technology, Rapid City, SD 57701, USA. [6]Department of Paleobiology, Smithsonian Museum of Natural History, Washington, DC 20560, USA. [7]Department of Geological Sciences, University of Colorado, Boulder, CO 80309, USA. [8]Department of Earth and Planetary Sciences, Northwestern University, Evanston, IL 60208, USA. [9]Department of Anthropology, University of Florida, Gainesville, FL 32611–7305, USA.

*To whom correspondence should be addressed. E-mail: rsecord2@unl.edu